Conductivity Relaxation and Chain Motions in Conjugated Conducting Polymers: Neutral Poly(3-alkylthiophene)s

Show-An Chen* and Chien-Shiun Liao

Chemical Engineering Department, National Tsing-Hua University, Hsinchu, Taiwan 30043, China

Received November 16, 1992; Revised Manuscript Received February 17, 1993

ABSTRACT: The conductivity relaxation behavior of neutral poly(3-alkylthiophene)s (P3ATs) with the alkyl side chain having carbon numbers 4, 6, 8, and 12 is investigated on the basis of dielectric relaxation measurements at −100 to 180 °C and 0.4–10^5 Hz after conversion to complex electric modulus formalism. It is found that the conductivity relaxation time distribution can be represented by the nonexponential decay function, $\varphi(t) = \exp(-t/\tau_p)^\beta$, involving a relaxation time distribution parameter β and a characteristic relaxation time τ_p as in the case of vitreous ionic inorganic conducting materials. The variation of relaxation time distribution with temperature is found to highly relate to the chain motions, with the aid of dynamic mechanical analysis and UV–vis spectroscopy. The side-chain motion gives no appreciable effect on the charge transport, while in the glass transition and rubbery region the relaxation time distribution becomes broadened with temperature. As the coplanar subchains in the ordered region melt, the conjugation length decreases and its distribution (and therefore relaxation time distribution) becomes narrower. As an electric field is applied, charges delocalized along coplanar subchains (each with one or two soft conformon terminals) hop over localized conformons to the neighboring sites. A contribution to the conductivity due to charge hopping across the side chains is insignificant, since its activation energy does not increase with the side-chain length.

Introduction

Indroducing a flexible side chain such as an alkyl group with a carbon number of 4 or more on the 3-position of the thiophene unit allows the intractable polymer to become soluble in common organic solvents, fusible, and melt processable, yet retain a rather high conductivity of about 30–100 S/cm after doping.[1] Two properties are of particular interest for the poly(3-alkylthiophene)s (P3ATs), viz., thermochromism and conductivity. The former resulted from a rod-to-coil transition of the main chains by raising the temperature to a level higher than their melt transition temperatures.[2] The thermochromism phenomenon of the P3ATs was also considered in a molecular level as a generation of twists (a disruption of coplanarity).[3] These conformational defects, which are termed "conformons", partition a polymer chain into subchains having a distribution of smaller conjugation length as evidenced by the blue shift of optical absorption maximum with increasing temperature.[4] For the charge transport mechanism, a variable range hopping model[5] is usually used for doped P3ATs at very low temperature (i.e., below −70 °C for poly(3-octylthiophene) with the doping level 0.2).[6] However, studies on effects of chain motions on charge transport behaviors are still lacking.

The relaxation of an electric field in a charge carrier system results from the charge hopping of mobile carriers over potential barriers, which can lead to short-range (or local) ac conductivity and long-range dc conductivity. Macedo et al.[7] have proposed the electric modulus formalism M^*, which is the inverse complex permittivity ($M^* \equiv 1/\epsilon^*$), to analyze conductivity relaxation due to the hopping motion of ions in vitreous ionic conductors such as $Ca(NO_3)_2/KNO_3$ (40/60 by mole). The conductivity relaxation in conjugated polymers arising from carrier hopping is different from the dielectric relaxation arising from a permanent dipole reorientation in conventional polymers. The electric modulus can be added in series like impedance formalism to describe the distribution of conductivity relaxation times and can depress the electrode polarization effect which often occurs in dielectric constant formalism.[7] Bakr et al.[8] and Emin and Ngai[9] have applied the electric modulus method to the conjugate polymers poly(arylenevinylene)s and *trans*-polyacetylene, respectively; for the former the electric field decay function was described by the nonexponential decay function $\exp[-(t/\tau_p)^\beta]$, where β is a parameter characterizing the relaxation time distribution and is 0.5 for this system and τ_p is the characteristic conductivity relaxation time.

This work reports on the conductivity relaxation of the neutral P3ATs and effects of thermal motions of the main chains and alkyl side chains at various temperature levels on the charge transport behavior by use of dynamic dielectric measurement, thermal analysis, and spectroscopic analysis (UV–vis). The P3ATs investigated include poly(3-butylthiophene) (P3BT), poly(3-hexylthiophene) (P3HT), poly(3-octylthiophene) (P3OT), and poly(3-dodecylthiophene) (P3DDT).

Experimental Section

Neutral P3ATs were prepared following the chemical method used by Sugimoto et al.[10] A 0.1 M 3-alkylthiophene monomer was oxidation-polymerized in a 0.4 M $FeCl_3$ solution in chloroform at room temperature under nitrogen atmosphere. The resulting mixture was then poured into methanol for precipitating out the polymer. This polymer was then washed several times with methanol and then extracted with methanol in a Soxhlet extractor to remove the residual oxidant and oligomers. The purified polymer was then dissolved in chloroform. The resulting solution was filtered to remove insoluble gels. Then the clear solution was cast in a Teflon mold to give a film with a thickness of about 0.125 mm. This thin film, after dynamic vacuum pumping until a constant weight was retained, was ready for physical characterizations. The P3HT so prepared has about 80% head-to-tail dyad and 20% head-to-head dyad as determined from ^1H NMR peaks[11,12] at δ 2.80 and 2.55 at room temperature in chloroform-*d* using a Bruker AM 400 MHz NMR spectrometer. The head-to-tail dyad content of the other P3ATs is expected to be 80% also, since it is insensitive to alkyl side chain length (C_6–C_{12}) of P3ATs if prepared by the same method.[11]

Ultraviolet–visible spectra (UV–vis) at −100 to 250 °C were recorded using an UV–vis spectrophotometer (Shimadzu Model UV-160). The spectrophotometer was equipped with a variable-temperature cell to allow measuring of spectra under vacuum

* Author to whom correspondence should be addressed.

0024-9297/93/2226-2810$04.00/0

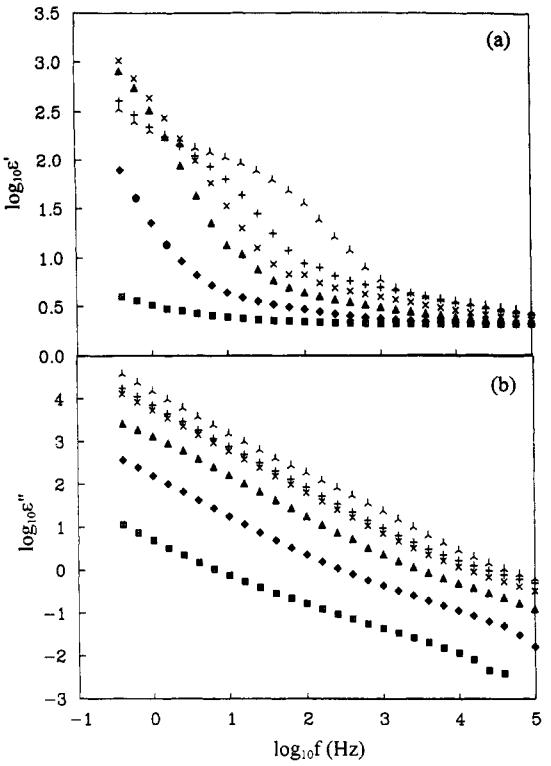

Figure 1. (a) Dielectric constant ϵ'; (b) dielectric loss ϵ'' vs $\log_{10} f$ for neutral poly(3-hexylthiophene) at −100 (■), −50 (◆), 0 (▲), 50 (×), 100 (+), and 150 °C (⅄).

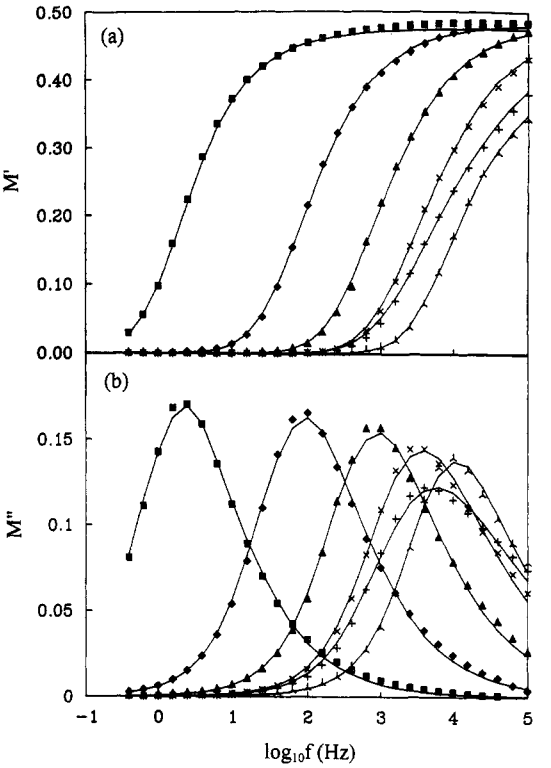

Figure 2. (a) Real part M'; (b) imaginary part M'' of the complex electric modulus M^* vs $\log_{10} f$ for neutral poly(3-hexylthiophene) at −100 (■), −50 (◆), 0 (▲), 50 (×), 100 (+), and 150 °C (⅄).

from −100 to 250 °C; the soaking time was 10 min at each specific temperature, and the heating rate used was about 1–2 °C/min during heating. The testing sample was prepared by coating P3AT solution in chloroform on a piece of quartz and allowing to dry to give a coated film with a thickness in the order of 1 μm.

A dynamic mechanical analyzer (Du Pont Model DMA983) was used to measure dynamic modulus (E' and E'') and loss tangent (tan δ) of the polymer films in the temperature range −150 to 200 °C at the heating rate of 2 °C/min and frequency of 1 Hz. The sample size was about 10 mm long, 2 mm wide, and 0.1 mm thick. After the sample was mounted in the sample chamber, the sample length subject to cyclic flexual motion was about 1 mm.

A dielectric analyzer (Du Pont Model DEA 2970, frequency range 0.03–10^5 Hz) was used to measure the dielectric constant ϵ' and dielectric loss ϵ'' of the polymer films in the frequency range from 0.4 to 10^5 Hz and the temperature range −100 to 180 °C under nitrogen gas purging. The sample size was about 25 mm × 25 mm × 0.125 mm. To ensure that the sample was bubble free and compressed tightly, the sample was mounted in between the parallel-plate electrodes and compressed with the force 300 N at 10 °C below its melting temperature for 10 min under dry nitrogen gas. Then the sample was slowly cooled to room temperature and was then ready for the dielectric measurement. In a comparative measurement for investigating the effect of electrode polarization, both surfaces of the sample were covered by polyimide thin films (Kapton, 0.02 mm thick) so that a dc current could not pass through from one electrode to the other.

Results and Discussion

1. Electric Modulus Analysis. Dynamic dielectric measurements for neutral P3BT, P3HT, P3OT, and P3DDT were performed. The real and imaginary parts of complex permittivity ϵ^*, the dielectric constant ϵ' and dielectric loss ϵ'', vs frequency for typical P3ATs, P3HT, at six representative temperatures in the range −100 to 150 °C are shown in Figure 1. Both ϵ' and ϵ'' increase with decreasing frequency at all temperature levels. The ϵ'' exhibits no loss peaks even at higher temperature and increases about linearly with decreasing frequency due to the increased contribution of dc conductivity, while ϵ' increases sharply with decreasing frequency below 10^3 Hz. The strong low-frequency dispersion for ϵ' and ϵ'' is characteristic of charged carrier systems.[13] The localized charge carriers under the applied alternating electric field can hop to neighboring localized sites like the reciprocating motion of a jumping dipole or jump to neighboring sites which form a continuous connected network, allowing the charges to travel through the entire physical dimensions of the sample and causing the electric conduction. Both processes suffer a time-delay response in the applied alternating electric field. During the motion of charge carriers, the applied electric field E will be subject to a decay. Such relaxation of E is termed electric field relaxation.[13]

To analyze the conductivity relaxation of the neutral P3ATs, the complex permittivity is converted to the complex electric modulus $M^*(\omega)$, according to the relation defined by Macedo et al.[7] The real and imaginary parts M' and M'' of the electric modulus can be calculated from ϵ' and ϵ'' via

$$M' = \frac{\epsilon'}{\epsilon'^2 + \epsilon''^2} \qquad M'' = \frac{\epsilon''}{\epsilon'^2 + \epsilon''^2} \tag{1}$$

M' and M'' of neutral P3HT converted from ϵ' and ϵ'' by eq 1 are shown in Figure 2. M' approaches zero at low frequencies, indicating that the electrode polarization gives a negligible contribution to M' and can be ignored when the permittivity data are expressed in this form.[7] In addition, each M'' curve shows a relaxation peak at the characteristic relaxation frequency f_{max}; f_{max} increases with increasing temperature, indicating that the conduction is a thermally activated process. The dispersions of M' and M'' indicate the presence of relaxation time distribution of conduction. The electric modulus M is a more convenient term in characterizing a decay of an applied electric field E due to charge motion in a conductor than ϵ, since M ($\equiv 1/\epsilon \equiv E/D$) is proportional to E, where D is the

dielectric displacement.[13] As a constant voltage is applied on the sample, the electric field in the sample decays as a function of time as $E(t) = E(0)\varphi(t)$, where $E(0)$ is the initial electric field and $\varphi(t)$ the decay function.

The complex permittivity can be represented as

$$\epsilon^* \equiv \epsilon'(\omega) - i\epsilon''(\omega) = \epsilon'(\omega) - i(\sigma(\omega)/\omega e_0) \quad (2)$$

where e_0 is the permittivity of free space (8.854×10^{-14} F/cm). If dc conductivity is appreciable

$$\epsilon''(\omega) = \epsilon''_{dc} + \epsilon''_{ac} = \sigma_{dc}/\omega e_0 + \sigma_{ac}(\omega)/\omega e_0 \quad (3)$$

where σ_{dc} and $\sigma_{ac}(\omega)$ are low-frequency limit conductivity and ac conductivity, respectively. For a conductor with a single conductivity relaxation time[7]

$$\epsilon^* = \epsilon_\infty - i(\sigma_{dc}/\omega e_0) \quad (4)$$

and

$$M^* = M_\infty\left(\frac{i\omega\tau_0}{1 + i\omega\tau_0}\right) = M_\infty\left[\frac{(\omega\tau_0)^2 + i\omega\tau_0}{1 + (\omega\tau_0)^2}\right] = M' + iM'' \quad (5)$$

where τ_0 is the conductivity relaxation time defined as $\tau_0 = e_0\epsilon_\infty/\sigma_{dc}$, M_∞ is the high-frequency limit of inverse ϵ' defined as $M_\infty = 1/\epsilon_\infty$, and ϵ_∞ is the high-frequency limit of dielectric constant. For a conductor with a distribution of conductivity relaxation times, the complex electric modulus $M^*(\omega)$ can be expressed by an extension of eq 5 as[14]

$$M^* = M_\infty\int_0^\infty g(\tau)d\tau\left(\frac{i\omega\tau}{1 + i\omega\tau}\right) = M_\infty\left[1 - \int_0^\infty g(\tau)d\tau\left(\frac{1}{1 + i\omega\tau}\right)\right] = M_\infty[1 - N^*(\omega)] \quad (6)$$

with

$$N^*(\omega) = N'(\omega) - iN''(\omega) \quad (7)$$

where $g(\tau)$ corresponds to a normalized distribution function of conductivity relaxation times resulting from a distribution of energy barrier heights for the carrier transport, with $\int_0^\infty g(\tau)d\tau = 1$. The decay function $\varphi(t)$ in time domain with the general form

$$\varphi(t) = \int_0^\infty g(\tau)\exp(-t/\tau)d\tau \quad (8)$$

can be used to describe the conductivity relaxation in the frequency domain by the Fourier transform[7]

$$M^* = M_\infty\left\{1 - L\left[\frac{-d\varphi(t)}{dt}\right]\right\} = M_\infty\left\{1 - \int_0^\infty dt\exp(-i\omega t)\left[\frac{-d\varphi(t)}{dt}\right]\right\} \quad (9)$$

where L denotes the Laplace transform. For describing a condensed matter with non-Debye relaxation, the Kohlrausch–Williams–Watts (KWW) nonexponential decay function[15]

$$\varphi(t) = \exp[-(t/\tau_p)^\beta], \quad 0 < \beta \le 1 \quad (10)$$

can be used satisfactorily, where τ_p is the characteristic conductivity relaxation time and β is a parameter characterizing the relaxation time distribution. When $\beta = 1$, the decay is exponential with a single conductivity relaxation time. When β decreases, the width of the relaxation time distribution increases. The analysis techniques developed by Moynihan et al.[14] are used to elucidate the conductivity relaxation with the use of the following summation expression to approximate the decay function in integal form as eq 8

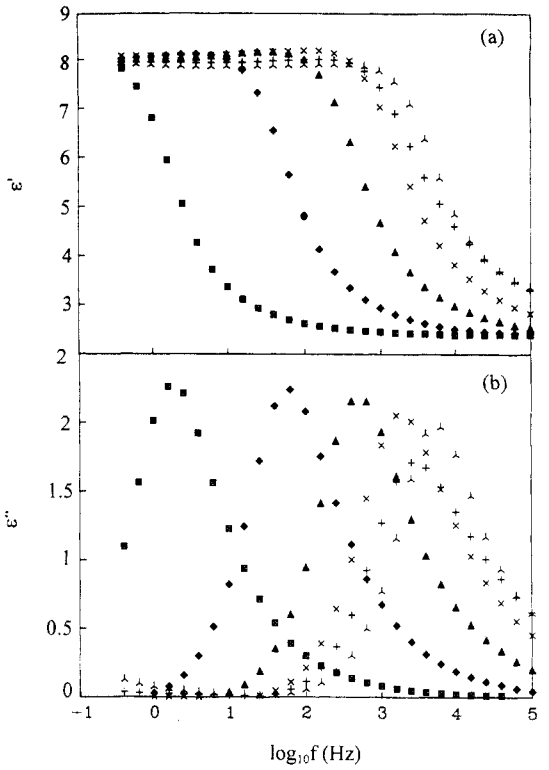

Figure 3. (a) Dielectric constant ϵ'; (b) dielectric loss ϵ'' vs $\log_{10} f$ for neutral poly(3-hexylthiophene) blocked by thin polyimide films at −100 (■), −50 (◆), 0 (▲), 50 (×), 100 (+), and 150 °C (⅄).

$$\varphi(t) = \sum_{i=1}^{n} g_i \exp(-t/\tau_i) \quad (11)$$

with $n = 18$ and then following with a direct evaluation of the Laplace transform of the approximated $\varphi(t)$ (eq 11) to fit the experimental data of M^*. In the fitting, the relaxation parameters M_∞, τ_p, and β were considered as fitting parameters. The deviation between the fitting curves (solid lines in Figure 2) and data is small. The dispersion or shape of the M'' curves depends on the value of β; greater deviation of β from 1 indicates a larger dispersion. The position of the peak, on the other hand, depends on τ_p; large τ_p gives a low characteristic relaxation frequency f_{max} ($f_{max} = 1/2\pi\tau_p$).

To confirm that the electric modulus formalism does eliminate the effect of electrode polarization, both surfaces of the sample were covered by polyimide thin films. The measured permittivity is shown in Figure 3. The dielectric constant ϵ' exhibits a low-frequency plateau corresponding to the bulk static dielectric constant ϵ_0, while the dielectric loss shows a loss peak characterized by a relaxation frequency f^P_{max} which is the same as that of the M'' curve at the same temperature. After the elimination of the effect of electrode polarization, the dielectric relaxation caused by a local hopping transition of charge carriers exhibits the same behavior as that of the conductivity relaxation. Thus, the electric modulus formalism is a convenient technique to analyze the conductivity relaxation in the π-conjugated systems. However, the characteristic relaxation frequency of the blocked P3HT, f^M_{max}, extracted from the data represented by the electric modulus formalism is lower than f^P_{max} by a factor of $\epsilon_0/\epsilon_\infty$

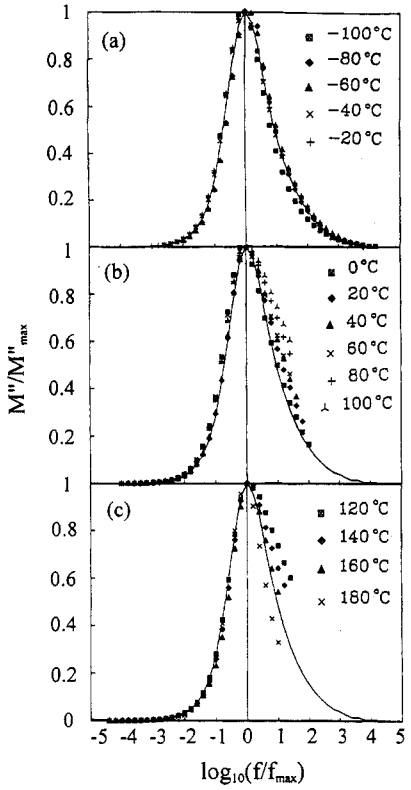

Figure 4. Reduced plot of M''/M''_{max} vs $\log_{10}(f/f_{max})$ for neutral poly(3-hexylthiophene) at (a) −100, −80, −60, −40, and −20 °C; (b) 0, 20, 40, 60, 80, and 100 °C; and (c) 120, 140, 160, and 180 °C.

according to the relationship[16]

$$\frac{f^{P}_{max}(\text{permittivity formalism})}{f^{M}_{max}(\text{modulus formalism})} = \frac{\epsilon_0}{\epsilon_\infty} = \frac{M_\infty}{M_0} \qquad (12)$$

where M_0 is the inverse of ϵ_0. Thus, as the sample is blocked by nonconducting materials so that no charge is transported from one electrode to the other, the f^{M}_{max} should be corrected by the factor $\epsilon_0/\epsilon_\infty$.

2. Conductivity Relaxation Time Distribution and Chain Motions at Various Temperature Levels. The reduced plots of M''/M''_{max} vs $\log_{10}(f/f_{max})$ for P3HT at various temperatures are shown in Figure 4. At the low-temperature range (−100 to −20 °C), the M''/M''_{max} curves almost locate on the same distribution curve (Figure 4a), indicating an existence of the same distribution of relaxation times and therefore the same β value. As temperature increases to the range 0–100 °C, the width of the distribution curves increases with increasing temperature as shown in Figure 4b. As temperature further increases to the range 120–180 °C, the distribution curves become narrower as shown in Figure 4c. The solid lines in Figure 4b,c are the fitted curve in Figure 4a for comparison purposes.

The calculated values of β from curve fitting at various temperatures for the P3ATs are plotted in Figure 5. Let us analyze the typical P3AT, P3HT, first. The variation of β with temperature can be divided into four regions: (i) below −30 °C, β remains constant at a value of about 0.61; (ii) between −30 and 40 °C, it drops significantly; (iii) between 40 and 100 °C, it drops rapidly; (iv) above 100 °C, it increases rapidly. The temperature dependence of the relaxation time distribution parameter β is highly related to the thermal transitions determined from mechanical relaxation and optical absorption (which reflects the conjugation length or energy of the π-electrons) experiments as to be revealed below.

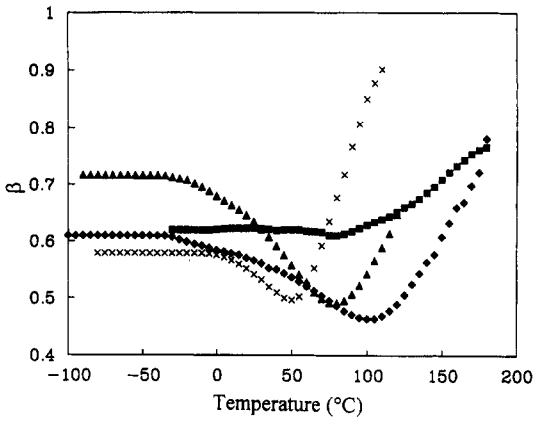

Figure 5. Variation of relaxation time distribution parameter β with temperature T for neutral poly(3-butylthiophene) (■), poly(3-hexylthiophene) (◆), poly(3-octylthiophene) (▲), and poly(3-dodecylthiophene) (×).

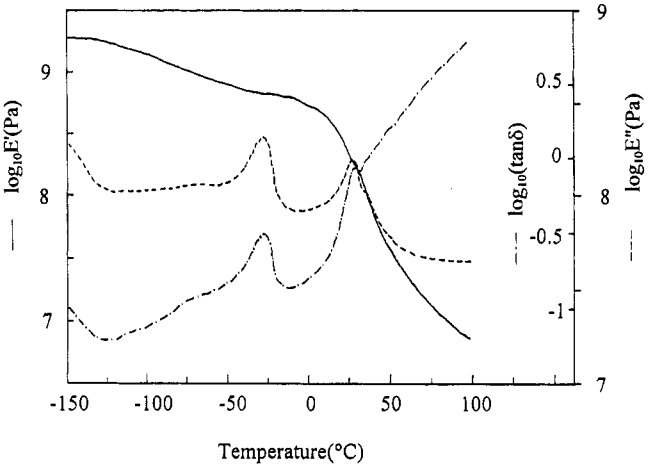

Figure 6. Dynamic mechanical analysis of neutral poly(3-hexylthiophene) at frequency of 1 Hz and heating rate of 2 °C/min.

The dynamic mechanical analysis (DMA) of P3HT in Figure 6 shows the following: (i) a β transition in the temperature range −125 to −15 °C (centered at −26 °C) resulting from a relaxation of the hexyl side chains; (ii) an α transition (glass transition) from −15 to 75 °C (centered at 27 °C) resulting from a relaxation of the conformons (twists in the disordered phase); (iii) a rubbery region between 75 and 100 °C; and (iv) above 100 °C the ordered phase in P3HT starts to melt.

The absorption maximum ($E_{\lambda max}$) vs temperature obtained from UV–vis spectra of the P3HT between −100 and 200 °C shown in Figure 7 can also be divided into three regions: (i) below −20 °C, $E_{\lambda max}$ remains constant at a value of about 2.46 eV; (ii) in the glass transition (a transition from soft conformons to more localized conformons) from −20 to 100 °C, $E_{\lambda max}$ increases by about 0.1 eV; and (iii) in the melting region from 100 to 180 °C, $E_{\lambda max}$ increases by 0.39 eV during which thermochromism occurs.

From a comparison among the analyses on the thermal transitions from the results of conductivity relaxation, DMA, and UV–vis spectra, it is quite clear that the conductivity relaxation behavior is highly related to the molecular motions. Below −30 °C (region i), although the side chains are relaxed while the main chains remain frozen, β remains constant, indicating that the side-chain motion has an insignificant effect on charge transport. As the subchains in the disordered phase (soft conformons) are able to relax (region ii), the torsion angle between two

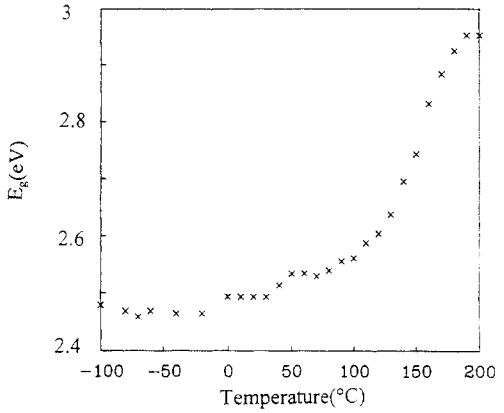

Figure 7. Variation of energy absorption maximum $E_{\lambda max}$ with temperature T for neutral poly(3-hexylthiophene).

successive rings in the conformons increases, leading to a decrease in conjugation length and an increase in the barrier height of charge carrier motion. Then the relaxation time distribution is broadened. As the temperature increases up to 100 °C (region iii), the torsion angle further increases and the conformons become more localized, causing the relaxation time distribution to be further broadened. As coplanar subchains in the ordered phase melt (region iv), the conjugation length becomes shorter and finally reaches a state of about two or three coplanar rings as the temperature reaches 190 °C, as calculated by Salaneck et al.,[4] and the relaxation time distribution of the bulk polymer becomes very narrow.

A similar analysis for the other P3ATs (P3BT, P3OT, and P3DDT) was also carried out. As side-chain length increases, the thermal transition of the entire β curve shifts toward lower temperature level as in the case of the energy of optical absorption maximum. Effects of chain motions due to temperature variation on conductivity relaxation behavior of the other P3ATs except P3BT are similar to those of P3HT. The β curve for P3BT is quite different from those of the others, in which β remains constant in the vicinity of α-transition region as in the case of its energy of optical absorption maximum.[17] The latter was attributed to the coupled thermal motions of the side chain and main chain owing to its shorter side chain, since no side-chain relaxation (β transition in DMA) and no transition shoulder in the energy of optical absorption maximum in the α-transition region are observed.

3. Conductivity Relaxation Behavior in the Glass Transition and Melting Regions. The temperature dependence of f_{max} for P3ATs is shown in Figure 8 in the form of the Arrhenius plot $\log_{10} f_{max}$ against $1/T$; the slope of the linear portions below the onset of the α-transition region (or the glassy state) is taken as the activation energy for conductivity relaxation $E_a^g(f_{max})$. The values of $E_a^g(f_{max})$ are in the range 0.19–0.38 eV (Table I), which is lower than the range 0.5–0.8 eV for the activation energies of side-chain relaxation of conventional polymers determined by dielectric relaxation.[13] The $E_a^g(f_{max})$ values for P3ATs decrease with increasing length of the alkyl side chains, indicating that the P3ATs with longer side chains should have lower energy barriers for charge hopping.

During the α-transition region, the curves of $\log_{10} f_{max}$ vs $1/T$ in Figure 8 are concave downward as in the case of dielectric relaxation and mechanical relaxation of conventional amorphous polymers and can fit the free volume model, the Williams–Landel–Ferry (WLF) equation,[18] quite well (the inset in Figure 8)

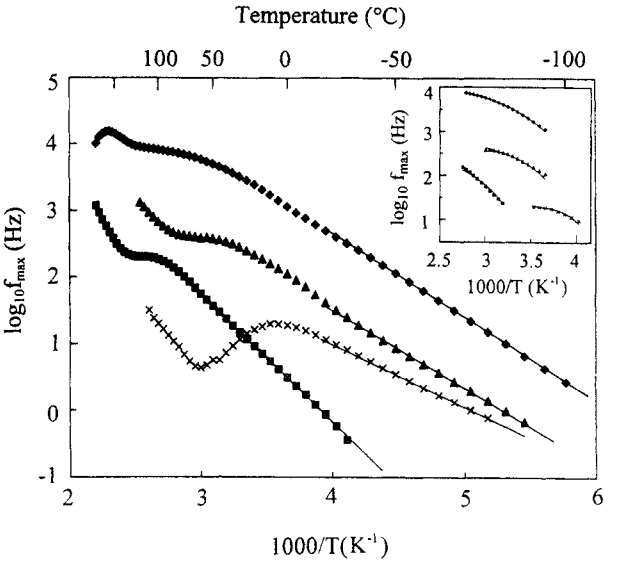

Figure 8. Variation of maximum relaxation frequency f_{max} with temperature T for neutral poly(3-butylthiophene) (■), poly(3-hexylthiophene) (◆), poly(3-octylthiophene) (▲), and poly(3-dodecylthiophene) (×). The inset is the relaxation rate for neutral P3ATs fitting by WLF equation at glass transition region.

Table I. Activation Energies of Conductivity Relaxation E_z^g (f_{max}) below the Onset of Glass Transition Regin and Williams–Landel–Ferry Parameters for P3ATs

	P3BT	P3HT	P3OT	P3DDT
$E_a^g(f_{max})$ (eV)	0.38	0.25	0.22	0.19
C_1	8.54	3.14	3.21	2.35
C_2	10.31	26.63	14.82	3.03
T_0 (°C)	−5.5	−30.4	−25.8	−35.0
f_g	0.051	0.138	0.135	0.185
α_f(10^{-3} °C^{-1})	4.93	5.19	9.13	61.0
T_α(onset)[a] (°C)	5	−15	−25	−25
T_m(onset)[a] (°C)	150	100	80	90
$E^g_{\lambda max}$[a] (eV)	2.59	2.46	2.44	2.42

[a] Onset temperatures of the α transition and melting regions for the P3ATs were determined from the energy of absorption maximum $E_{\lambda max}$ vs temperature and for P3BT, P3OT, and P3DDT were taken from ref 17. $E^g_{\lambda max}$ is the value of $E_{\lambda max}$ at −100 °C.

$$\log\frac{f_{max}(T)}{f_{max}(T_0)} = \log\frac{1}{a_T} = \frac{C_1(T-T_0)}{C_2+(T-T_0)} \qquad (13)$$

where $f_{max}(T_0)$ is the relaxation frequency at the reference temperature T_0 and C_1 and C_2 are fitting parameters. According to the WLF theory,[19] these parameters are related to the fractional free volume below the reference temperature f_g and the free volume expansion coefficient above the reference temperature α_f as

$$f_g = [C_1 \ln(10)]^{-1} \quad \text{and} \quad \alpha_f = f_g/C_2 \qquad (14)$$

The fitting parameters T_0, C_1, and C_2 and the calculated f_g and α_f are listed in Table I. T_0 is about 10–15 °C lower than the onset temperature of the α transition, while the values of f_g and α_f are larger than the "universal" values 0.025 and 4.8×10^{-4} determined from mechanical relaxation, respectively. This might indicate that the fractional free volume for charge hopping at glassy state is larger than that for displacement of dipoles in conventional polymers. The f_g in the latter only corresponds to the free volume around the orientational dipoles, while f_g in the former can be interpreted as the volume within which a charge can freely hop to its near-neighboring sites. The present α_f for charge hopping is 1–2 orders higher than the α_f determined from mechanical relaxation. This can

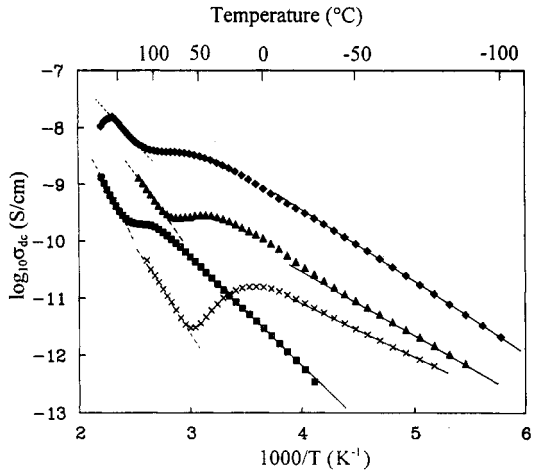

Figure 9. Plot of $\log_{10}\sigma_{dc}$ vs T^{-1} for neutral poly(3-butylthiophene) (■), poly(3-hexylthiophene) (◆), poly(3-octylthiophene) (▲), and poly(3-dodecylthiophene) (×).

Table II. Activation Energies of σ_{dc} in the Glassy State $E_a^g(\sigma_{dc})$ and the Melt State $E_a^m(\sigma_{dc})$ for P3ATs

	P3BT	P3HT	P3OT	P3DDT
$E_a^g(\sigma_{dc})$ (eV)	0.38	0.25	0.22	0.19
$E_a^m(\sigma_{dc})$ (eV)	0.74	0.41	0.59	0.54

probably be attributed to the fact that charge mobility is much more thermally sensitive than segment mobility. The fit of f_{max} vs T with the WLF equation for conductivity relaxation in the glass transition region indicates that the increase of ring distortion (or increase of localization of the conformons) in the disordered region does affect the conductivity relaxation behavior.

From the conductivity relaxation data, dc conductivity σ_{dc} can be estimated from the relaxation parameters as[14]

$$\sigma_{dc} = e_0/M_\infty\langle\tau_p\rangle \tag{15}$$

where $\langle\tau_p\rangle$ is the average relaxation time. For a decay function defined by eq 10, $\langle\tau_p\rangle$ is given by[14,20]

$$\langle\tau_p\rangle = \int_0^\infty dt\varphi(t) = \frac{\tau_p}{\beta}\Gamma\left(\frac{1}{\beta}\right) \tag{16}$$

where Γ denotes the gamma function. The calculated σ_{dc} values for the P3ATs are plotted against inverse temperature $1/T$ as shown in Figure 9; the variations of σ_{dc} and f_{max} (Figure 8) with $1/T$ are very close. In the same way as f_{max}, σ_{dc} also increases linearly with increasing temperature below the onset of the glass transition region, shows a drastic change in the α-transition region, and then again increases linearly during melting of the ordered phase with increasing temperature. The activation energies of σ_{dc} in the glassy state $E_a^g(\sigma_{dc})$ and in the melt state $E_a^m(\sigma_{dc})$ evaluated by Arrhenius relation are listed in Table II; the former is about half of the latter. This remarkable change of σ_{dc} for the P3ATs was also observed by Yoshino et al.[21] using direct measurement of dc conductivity. They attributed this change to strong carrier scattering due to large conformation change at the maximum conductivity temperature,[21] which decreased with increasing alkyl chain length as is also observed in this work. However, no specific description about the conformation change was given by them. In addition, for poly(3-docosylthiophene), they observed a conductivity maximum at solid–liquid transition temperature at about 75 °C.[22]

4. Charge Transport Path. In our previous work,[17] it was established that, before the onset of glass transition of the P3ATs, the conformational defects in the main chains are soft conformons, in which the distortion is distributed over several repeating units between two successive coplanar subchains or between a coplanar subchain and a localized conformon. The torsion angle in the soft conformon would be sufficiently small to allow π electrons in the soft conformon to participate in the delocalization with their immediate neighboring coplanar subchains of the same chain. The energy of optical absorption maximum below the onset of the glass transition region $E^g_{\lambda max}$ of the P3BT, P3HT, P3OT, and P3DDT (each varies by about 0.015 eV and can be considered as a constant) are 2.59, 2.46, 2.44, and 2.42 eV at −100 °C respectively. The decrease of $E^g_{\lambda max}$ with increasing side-chain length, which can promote the extent of coplanarity in the soft conformons and conjugation length in the coplanar subchains, is in agreement with the case of E_a^g (σ_{dc}). Thus, the charge transport path can be inferred: a charge first delocalizes along a coplanar subchain and its immediate neighboring conformon in the same chain and then hops over a neighboring localized conformon to a neighboring site in a coplanar subchain/soft conformon located in the same chain or in the other neighboring chains. A contribution to the conductivity due to interchain charge hopping across side chains is insignificant; otherwise, $E_a^g(\sigma_{dc})$ should increase with increasing alkyl side chain length. Under an applied alternating electric field, the localized carriers can hop to neighboring sites like the reciprocating motion of a jumping dipole (which contributes to ac conductivity) or jump to neighboring sites which form a continuous connected network, allowing the charges to travel through the entire physical dimensions of the sample (which contributes to dc conductivity). The high $E_a^g(\sigma_{dc})$ value of P3BT is due to its more localized conformons as can be manifested from its higher $E^g_{\lambda max}$ than the others.

In the glass transition region, as temperature increases, the torsion angle in the soft conformons increases. Thus, the previously delocalized π electrons in the soft conformons are confined to the localized subchains (localized conformons), causing an increase of the energy barrier of charge hopping. During this period of α relaxation, σ_{dc} exhibits a drastic change with temperature resulting from two competing factors of thermally activated charge motion (which leads to an increase in σ_{dc}) and increasing ring torsion angle in the conformons (which leads to a decrease in σ_{dc}). After the completion of the α-relaxation process, the coplanar subchains in the ordered phase start to melt. This leads to a shortening of the conjugation length and an increase of distance between localized sites. Thus, charge hopping must overcome the higher energy barrier as indicated by the larger activation energy as shown in Table II.

Conclusion

The complex electric modulus is a convenient formalism to eliminate the effect of electrode polarization in dielectric relaxation measurements of the conjugated polymers, from which information about conductivity relaxation behavior can be obtained. The conductivity relaxation time distribution can be represented by a nonexponential decay function involving a relaxation time distribution parameter and a characteristic relaxation time as in the case of vitreous ionic conducting materials. The variation of relaxation time distribution with temperature is highly related to the chain motions. As an electric field is applied, charges delocalized along coplanar subchains, each with one or two soft conformon terminals, hop over localized

conformons to the neighboring sites. Contribution to the conductivity due to charge hopping across the side chains is insignificant, since the activation energy does not increase with the side-chain length.

Acknowledgment. We thank the National Science Council of ROC for financial aid through the project Studies on Soluble Conjugated Polymers: Structural/Properties and Electrochemical Phenomena, NSC 81-0416-E007-04.

References and Notes

(1) Jen, K. Y.; Miler, G. G.; Elsenbaumer, R. L. *J. Chem. Soc., Chem. Commun.* **1986**, 1346.
(2) Winokur, M. J.; Spiegel, D.; Kim, Y.; Hotta, S.; Heeger, A. J. *Synth. Met.* **1989**, *28*, C419.
(3) Inganäs, O.; Salaneck, W. R.; Österholm, J.-E.; Laakso, J. *Synth. Met.* **1988**, *22*, 395.
(4) Salaneck, W. R.; Inganäs, O.; Thémans, B.; Nilsson, J.-O.; Sjögren, B.; Österholm, J.-E.; Brèdas, J.-L.; Svensson, S. *J. Chem. Phys.* **1988**, *89*, 4613.
(5) Mott, N. F.; Davis, E. A. *Electronic Processes in Non-Crystalline Materials*; Claredon Press: Oxford, U.K., 1979.
(6) Ishikawa, H.; Xu, X.; Kobayashi, A.; Satoh, M.; Suzuki, M.; Hasegawa, E. *J. Phys. D: Appl. Phys.* **1992**, *25*, 897.
(7) Macedo, P. B.; Moynihan, C. T.; Bose, R. *Phys. Chem. Glasses* **1972**, *13*, 171.
(8) Bakr, A. A.; North, A. M.; Kossmehl, G. *Eur. Polym. J.* **1977**, *13*, 799.
(9) Emin, D.; Ngai, K. L. *J. Phys., Colloq.* **1983**, *44*, C3-471.
(10) Sugimoto, R.; Takeda, S.; Gu, H. B.; Yoshino, K. *Chem. Express* **1986**, *1*, 635.
(11) Leclerc, M.; Diaz, F. M.; Wegner, G. *Makromol. Chem.* **1989**, *190*, 3105.
(12) Sato, M.; Morri, H. *Macromolecules* **1991**, *24*, 1169.
(13) Jonscher, A. K. *Dielectric Relaxation in Solids*; Chelsa Dielectric Press: London, 1983.
(14) Moynihan, C. T.; Boesch, L. P.; Laberge, N. L. *Phys. Chem. Glasses* **1973**, *14*, 122.
(15) Williams, G.; Watts, D. C. *Trans. Faraday Soc.* **1970**, *66*, 80.
(16) Lamb, J. *Rheol. Acta* **1973**, *12*, 438.
(17) Chen, S.-A.; Ni, J.-M. *Macromolecules* **1992**, *25*, 6081.
(18) Williams, M. L.; Landel, R. F.; Ferry, J. D. *J. Am. Chem. Soc.* **1955**, *77*, 3701.
(19) Aklonis, J. J.; MacKnight, W. J. *Introduction to Polymer Viscoelasticity*, 2nd ed.; Wiley: New York, 1983.
(20) Douglas, R. W. In *Amorphous Materials*; Douglas, R. W., Ellis, B., Eds.; Wiley-Interscience: London, 1972.
(21) Yoshino, K.; Park, D. H.; Park, B. K.; Fujii, M.; Sugimoto, R. *Jpn. J. Appl. Phys.* **1988**, *27*, L1410.
(22) Yoshino, K.; Park, D. H.; Onoda, M.; Sugimoto, R. *Solid State Commun.* **1988**, *67*, 1119.